Supplementary Information: Molecular electrometer and binding of cations to phospholipid bilayers†

Andrea Catte,[a‡] Mykhailo Girych,[b] Matti Javanainen,[c,d] Claire Loison,[e] Josef Melcr,[f] Markus S. Miettinen,[g,h] Luca Monticelli,[i] Jukka Määttä,[j] Vasily S. Oganesyan,[a] O. H. Samuli Ollila,[*b] Joona Tynkkynen,[c] and Sergey Vilov,[e]

1 Ion binding equilibration times

Simulations containing 450 mM $CaCl_2$ with CHARMM36 and Slipids were ran 2 μs to estimate the times required to equilibrate amount of bound Ca^{2+} in lipid bilayer. The amount of the bound calcium as a function of simulation time from these simulations are shown in Fig. S1. The results show clear increase in binding affinity up to 1000 ns and 700 ns in CHARMM36 and Slipids, respectively, and moderate increase even after this. This is also reflected to the CHARMM36 results in Fig. 2 in the main text, where long CHARMM36 simulation with 450 mM $CaCl_2$ show relatively lower order parameters than shorter simulations. This can be rationalised with higher and more equilibrated binding affinity in long simulations. The results suggest that in other simulations the binding affinity is underestimated due to the insufficient equilibration times. This should be taken into account in more careful studies, but do not interfere the conclusion in this work that Ca^{2+} binding is most likely overestimated in all the other models than CHARMM36 with ion model by Yoo et al.[1].

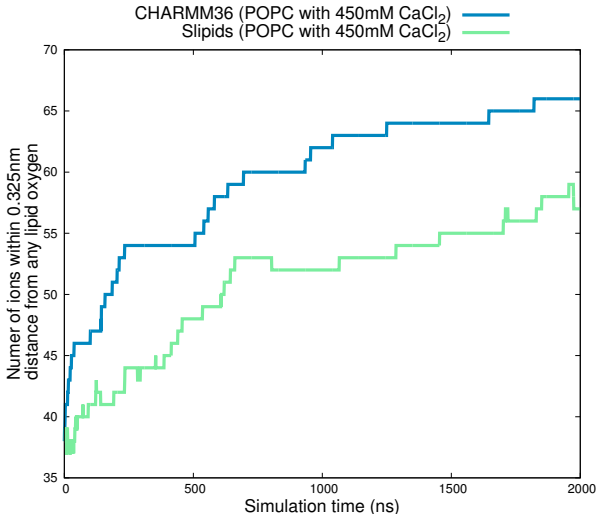

Fig. S1 Number of bound Ca^{2+} as a function of time from 2 μs long simulations with CHARMM36 and Slipids.

2 Change of choline order parameters as a function of bound cation charge

To demonstrate that also in current MD simulations the molecular electrometer works as Seelig and coworkers proposed in the 1980's (that is, there is a direct relationship between the changes in the choline β and α segment order parameters and the amount of penetrated charge), we calculated the bound cation charge and the corresponding order parameter change separately for each leaflet in several MD simulation systems.

As in reality ions have continuum density distributions, any division to bound and non-bound ions is somewhat artificial, and thus the choice of parameters describing ion partitioning is more or less ambiguous. We chose to integrate the cation charge distribution from the centre of the membrane until a certain predefined limit. Three limits were tested: until the g_3-carbon (Fig. S2), until the phosphorus (Fig. 3 in the main text), and until the α-carbon (Fig. S3) density maximum. Although phosphorus seems to be the most intuitive choice, comparison of these three plots shows that the conclusions we draw here do not depend on the chosen limit. That said, we must stress that the slopes of the curves de-

[a] *University of East Anglia, Norwich, United Kingdom*
[b] *Department of Neuroscience and Biomedical Engineering, Aalto University, Espoo, Finland*
[c] *Tampere University of Technology, Tampere, Finland*
[d] *University of Helsinki,Finland*
[e] *Institut Lumiére Matiére, UMR5306 Université Lyon 1-CNRS, Université de Lyon, 69622 Villeurbanne, France*
[f] *Institute of Organic Chemistry and Biochemistry, Czech Academy of Sciences, Flemingovo nám. 2, 16610 Prague 6, Czech Republic, Charles University in Prague, Faculty of Mathematics and Physics, Ke Karlovu 3, 121 16 Prague 2, Czech Republic*
[g] *Fachbereich Physik, Freie Universität Berlin, Berlin, Germany*
[h] *Max Planck Institute of Colloids and Interfaces, Department of Theory and Bio-Systems, Potsdam, Germany*
[i] *Institut de Biologie et Chimie des Protéines (IBCP), CNRS UMR 5086, Lyon, France*
[j] *Aalto University, Espoo, Finland*
[*] **Author to whom correspondence may be addressed. E-mail: samuli.ollila@aalto.fi.**
† Electronic Supplementary Information (ESI) available: 5 figures, detailed technical discussion and simulation details. See DOI: 10.1039/b000000x/
‡ The authors are listed in alphabetical order.

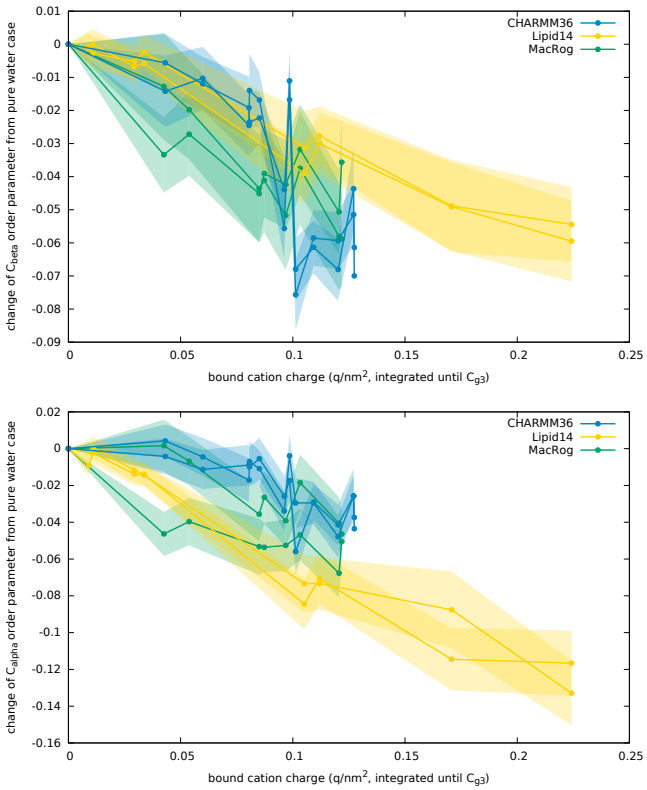

Fig. S2 Change of order parameters (from salt-free solution) of the β and α segments, $\Delta S^{\beta}_{\mathrm{CH}}$ and $\Delta S^{\alpha}_{\mathrm{CH}}$, shown as a function of bound cation charge. The order parameters as well as the bound charge calculated separately for each leaflet; **cations residing between the bilayer centre and the density maximum of g_3 carbon considered bound**; error bars show standard error of mean over lipids.

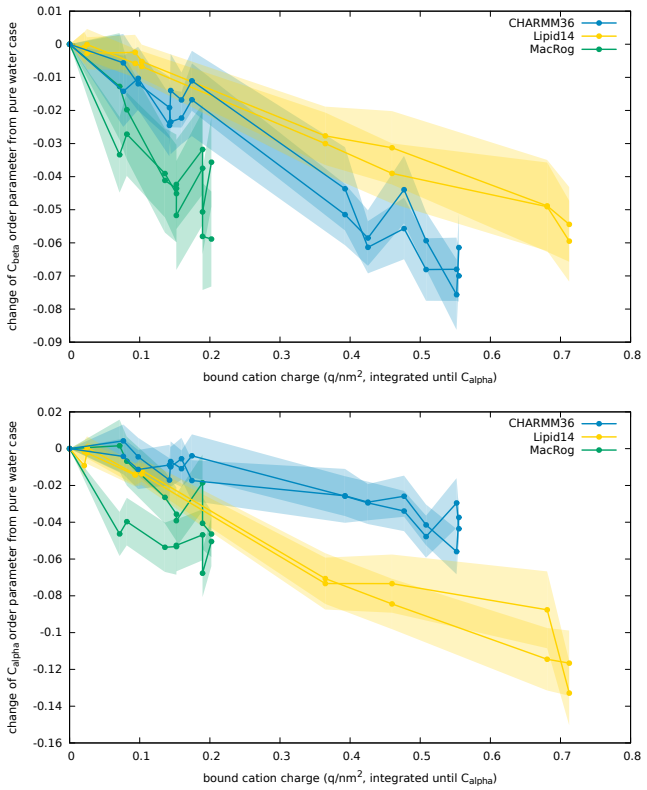

Fig. S3 Change of order parameters (from salt-free solution) of the β and α segments, $\Delta S^{\beta}_{\mathrm{CH}}$ and $\Delta S^{\alpha}_{\mathrm{CH}}$, shown as a function of bound cation charge. The order parameters as well as the bound charge calculated separately for each leaflet; **cations residing between the bilayer centre and the density maximum of α carbon considered bound**; error bars show standard error of mean over lipids.

pend **strongly** on the chosen limit; therefore, one should be very careful when comparing them to one another or to experimental data — a given limit might or might not match with what is considered 'bound' in an experiment.

Figures S2, S3 and 3 in the main text show that in all MD models a clear correlation exists between the bound cation charge and the change of the (β, α) order parameters. Also, this correlation does not seem to depend heavily on ion type, as Na^+ and Ca^{2+} fall effectively on the same line in each force field. In other words, the plots demonstrate that the molecular electrometer is robust, that is, qualitatively reproduced also in MD simulations, and even with rather inaccurate force fields. (A similar robust effect was the reorientation of the headgroup upon dehydration in our previous paper[2].)

We wish to note that with the mono- and divalent ions the bound charge is localised differently in the membrane. Interestingly, however, it seems that a single linear slope can capture responses to both. This is somewhat surprising, as one might expect correlation effects between the bound ions to show; probably these will become evident only at higher concentrations.

3 Headgroup response to charged amphiphiles

The order parameter changes as a function of the bound charge cannot be straightforwardly compared between simulations and experiments from systems with ions because the results depend on the definition of bound ions in simulations (see previous section). In systems with charged amphiphiles the situation is more straightforward since all the charges can be assumed to locate in bilayer in both, simulations and experiments. The order parameter changes as a function of charged amphiphiles, calculated from previously published simulation data[3–6] and experiments[7,8], is shown in Fig S4.

The simulation data is from previously published binary mixture of cationic dimyristoyltrimethylammoniumpropane (DMTAP) and zwitterionic (neutral) dimyristoylphosphatidylcholine (DMPC)[3–6], simulated with Berger based model. The experimental data from various amphiphiles with saturated acyl chains[7] show steeper slope than the data from from DMPC/DOTAP mixtures[8]. The origin of the difference is not known. It may arise, e.g., from the differences in acyl chain saturation level or headgroups of the amphiphiles. In the used simulation data the amphiphile acyl chains are fully saturated as in experimental data for various amphiphiles from Ref. 7, but the amphiphile head-

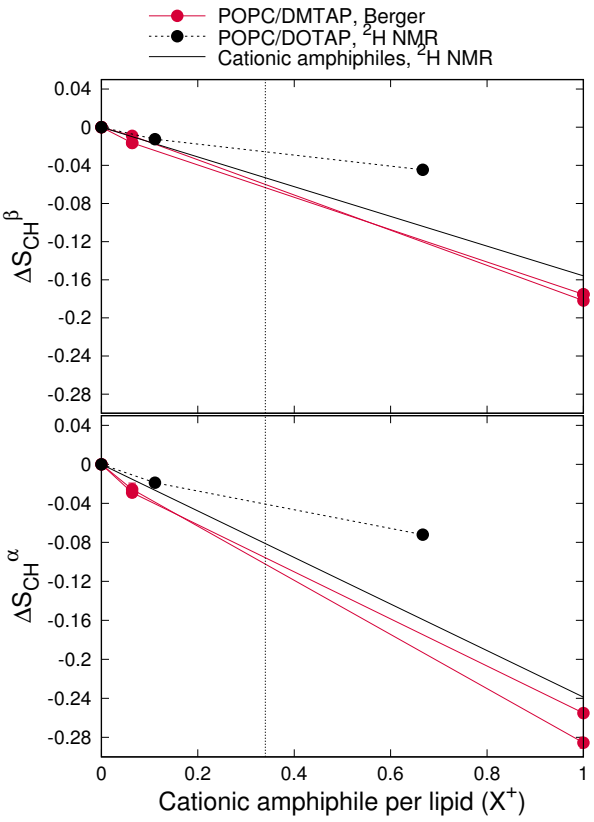

Fig. S4 Order parameter changes as a function of cationic amphiphiles from simulations[3–6] and experiments[7,8]. Experimental points for binary mixtures of POPC and 1,2-dioleoyloxy-3-(trimethylammonio)propane (DOTAP) are from [8]. Experimental lines are from $\Delta S^i_{\mathrm{CH}} = \frac{4}{3}\chi^{-1} m_i X^{\pm}$, where m_i are taken as average for different amphiphiles measured in 7.

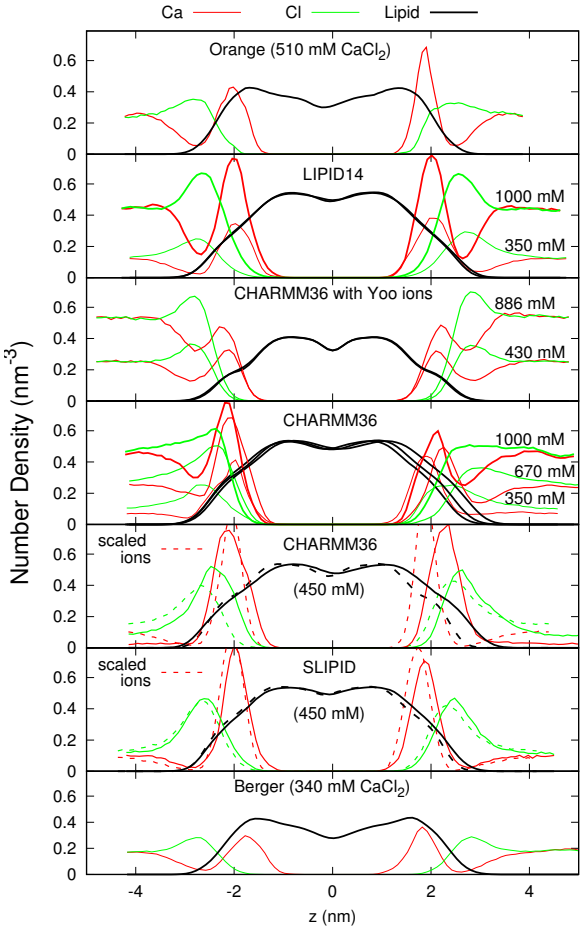

Fig. S5 Number density profiles for lipids, Ca^{2+} and Cl^- ions from simulations with different force fields and different $CaCl_2$ concentrations. The lipid densities are scaled with 100 (united atom) or 200 (all atom model) to make them visible with the used y-axis scale. The Cl^- density is scaled with 2 to equalise charge density of ions.

group and lipids are the same as in experimental data from Ref. 8. The order parameter changes from simulations overestimate the changes measured in latter experiment (especially with larger amphiphile concentrations), but are in good agreement with the former. However, the simulated system is not exactly the same as in experiments and also, the potential effect of Cl^- binding affinity cannot be excluded. Thus, with the available data we cannot accurately determine how realistic the headgroup response to bound charge is in simulation.

To estimate the maximum error we take the maximum amount of bound charge from Fig. 3 in the main text ($\approx 0.5 \frac{\mathrm{e}}{\mathrm{nm}^2}$) and assume the area per lipid of 0.68 nm^2. This gives for maximum amount of bound charge per lipid $X^+_{\mathrm{max}} = 0.5 \frac{\mathrm{e}}{\mathrm{nm}^2} \cdot 0.68 \frac{\mathrm{nm}^2}{\mathrm{lipid}} = 0.34 \frac{\mathrm{e}}{\mathrm{lipid}}$, which is shown as dashed line in Fig. S4. The maximum overestimations of order parameter decrease with this amount of bound charge per lipid are ≈0.04 and ≈0.06 for β and α order parameter changes, respectively. The numbers are smaller with less amount of bound cations. In principle, these values could explain the overestimated order parameter change due to the presence of $CaCl_2$ in Berger model but not in the presence of NaCl (see Fig. 2 in the main text).

In conclusion, with the current data we cannot fully exclude the possibility that the overestimated order parameter response to the $CaCl_2$ with Berger model arises from oversensitive headgroup response to bound cations. However, in the presence of NaCl the differences between responses in simulations and experiments in Fig. 2 in the main text are larger than the maximum estimated influence from a possible oversensitivity of the headgroup.

4 Density distributions with different $CaCl_2$ concentrations

The density distributions with all simulated $CaCl_2$ concentrations are shown in Fig. S5.

5 Effect of ion model and polarization

It has been suggested that the missing electronic polarizability can be compensated by scaling the ion charge in simulations[9]. To test if this would improve the Na^+ ion binding behaviour, we ran simulations with Berger-DPPC-97, BergerOPLS-DPPC-06 and Slipids with scaled Na^+ and Cl^- ions. For Berger-DPPC-97 and BergerOPLS-DPPC-06 models the ion charge in systems listed in Table 1 in the main text was simply scaled with 0.7 and the related files are available at [12–15]). For simulations with Slipids the ion model by Kohagen et al. was used[16] and the related files are available at[17]. The simulation parameters were identical to

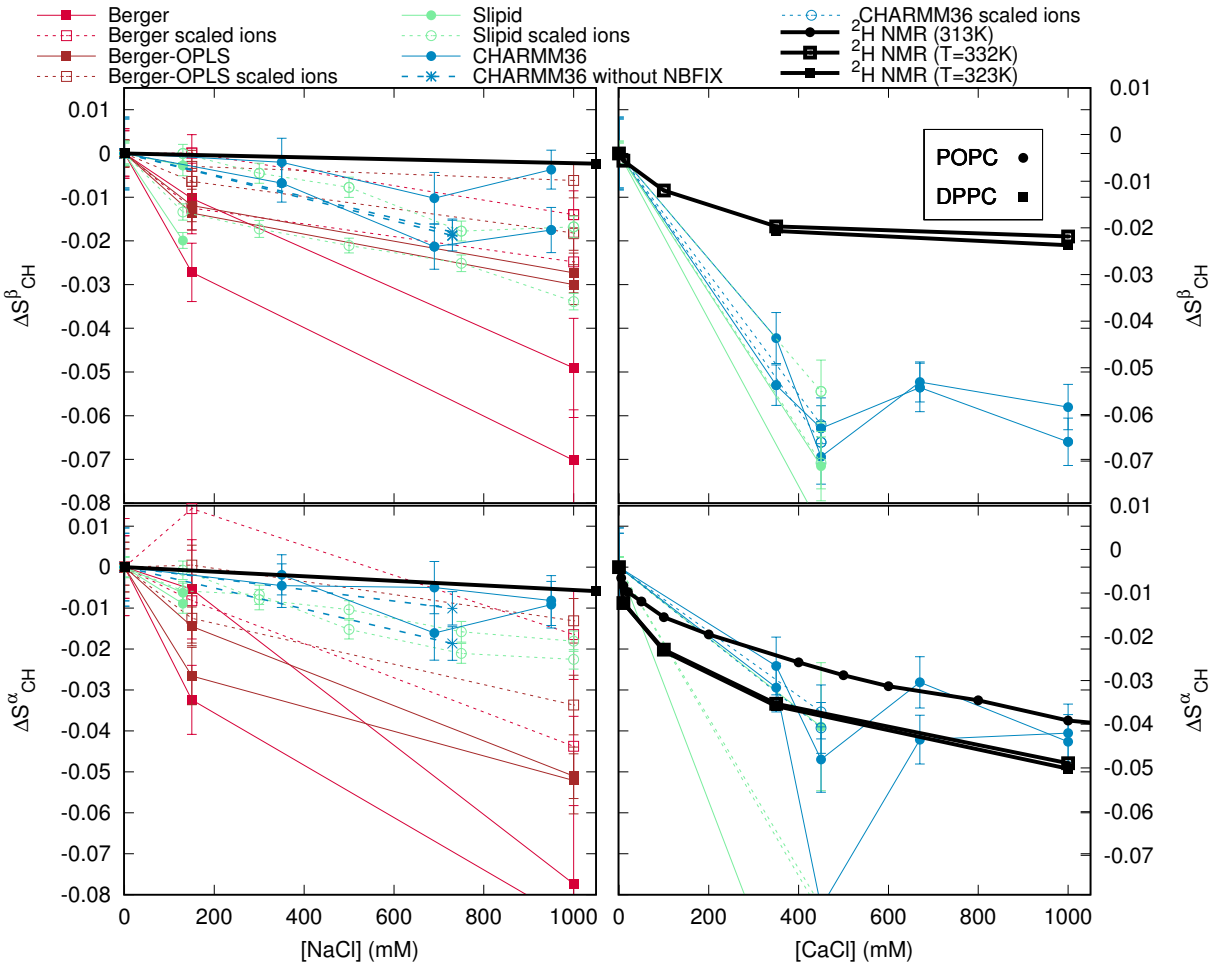

Fig. S6 The effect of charge scaling[9,10] and NBFIX[11] on order parameter changes in simulations.

those employed in the simulation of POPC with 130 mM NaCl (see Methods). The order parameter changes and Na^+-binding affinity are decreased by the charge scaling but yet overestimated with respect to the experiments as seen from Figs. S6 and S7. Thus the overestimated binding affinity cannot be fixed by only scaling the charges of ions.

The ion model for $CaCl_2$ with scaled charges[10] was tested with CHARMM36 and Slipid models. The related files are available at Refs. 18 and 19, respectively, and the results are shown in Figs. S5 and S6. The results with scaled charges are slightly improved but yet far from experiments.

Also the effect of NBFIX[11] on Na^+ binding in CHARMM36 is quantified. The simulation data without NBFIX is available at[20]. As expected, Figs. S6 and S7 show more significant order parameter decrease and higher Na^+ binding affinity without NBFIX. Thus, also the CHARMM36 model without NBFIX overestimates the Na^+ binding in PC bilayer.

6 Methods

6.1 Simulated systems

All simulations are ran with a standard setup for planar lipid bilayer in zero tension with periodic boundary conditions with Gromacs (version numbers 4.5-X-5.0.X)[21,22] or NAMD[23] software packages.

6.2 Analysis

The order parameters were calculated from simulation trajectories directly applying the equation $S_{\mathrm{CH}} = \langle \frac{3}{2}\cos^2\theta - \frac{1}{2} \rangle$, where θ is the angle between a given C–H bond and the bilayer normal, and the average is taken over all lipids and time frames. For united atom models, the positions of hydrogen atoms were calculated for each molecule in each frame *a posteriori* by using the *g_protonate* tool in Gromacs 4.0.2[24]. The statistical error in the order parameter was estimated by calculating the average value separately for each lipid molecule, and then the average and standard error of the mean over the ensemble of lipids (as done also in previous work[2]). All the scripts used for analysis and the resulting data are available in the GitHub repository[25]

6.3 Simulation details

6.3.1 Berger

POPC: The simulation without ions is the same as in Ref. 26 and the files are available at Ref. 27. The starting structures for simulations with ions is made by replacing water molecules with appropriate amount of ions (see Table 1 in the main text). The

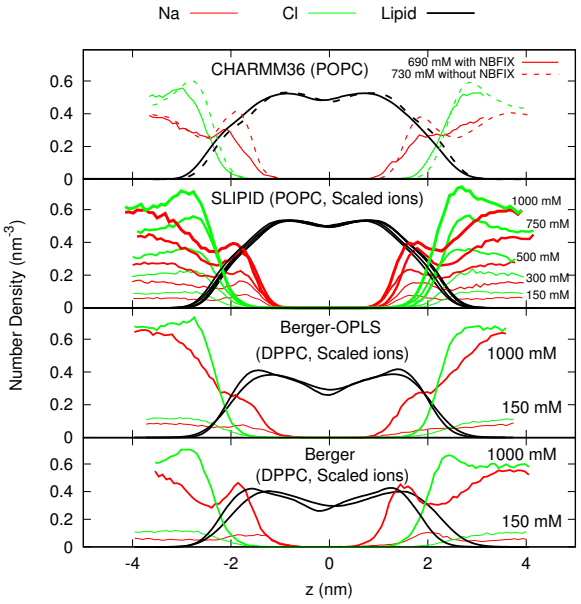

Fig. S7 Atom number density profiles along membrane normal coordinate z for lipids, Na^+ and Cl^- ions. The effect of NBFIX[11] on CHARMM36 simulation results is shown in top and other figures show the effect of ion models with scaled charges. The lipid densities are scaled with 100 (united atom) or 200 (all atom model) to make them visible with the used y-axis scale.

Berger force field was used for the POPC[28], with the dihedral potential next to the double bond taken from[29]. The ion parameters from ffmgx[30] were used. Timestep of 2 fs was used with leap-frog integrator. Covalent bond lengths were constrained with LINCS algorithm[31,32]. Coordinates were written every 10 ps. PME[33,34] with real space cut-off at 1.0 nm was used for electrostatics. Plain cut-off was used for the Lennard-Jones interactions with a 1.0 nm cut-off. The neighbour list was updated every 5th step with cut-off at 1.0 nm. Temperature was coupled separately for lipids, water and ions to 298 K with the velocity-rescale method[35] with coupling constant 0.1 ps^{-1}. Pressure was semi-isotropically coupled to the atmospheric pressure with the Parrinello–Rahman barostat[36].

DPPC: The simulation without ions is the same as in[2] and the files are available at[37]. The initial configuration contained 72 DPPC lipids and 2880 SPC water molecules. The standard Berger DPPC force field was used [28] (simulations indicated as Berger-DPPC-97 in Table 1 in the main text). The electrostatics were handled with PME[33,34], with real-space Coulomb cut-off set at 1.0 nm. Lennard-Jones potentials were cut off at 1.0 nm. The neighbour list for all non-bonded interactions was updated every 10 steps. Temperature was set to 323K with the velocity-rescale method[35] using a coupling constant of 0.1 ps^{-1}. Semi-isotropic pressure coupling at 1 atm was handled with the Parrinello-Rahman barostat[36] with 1 ps coupling constant. The time step was 4 fs, and coordinates were written every 10 ps. The total simulation time was 120 ns (without pre-equilibration) and last 60 ns was used in the order parameter analysis.

For simulations with added salt, the appropriate number of SPC water molecules were randomly replaced with ions. Ions were described by the ffgmx parameters[30]. In simulations with scaled charges, charge-scaling was applied by scaling the ion charges by a factor 0.7. Conditions in the ion simulations were as with the pure DPPC described above. The duration of the simulations was 120 ns (without pre-equilibration) and last 60 ns was used in the order parameter analysis.

All the simulation files for pure DPPC simulations can be found at Ref. 37 and for the simulations with ions at Refs. 38,39 and with scaled ions at Refs. 12,13.

6.3.2 BergerOPLS

For simulations without ions, the initial configuration contains 72 DPPC lipids and 2880 SPC water molecules. For simulations with added salt, the appropriate amount of SPC water molecules were randomly replaced with ions. The number of ions is reported in Table 1 in the main text. For the lipids, we used the same version of Berger force field as in previous simulations, described in[28]; for the ions, we used the Åqvist parameters[40] (commonly used within the OPLS-AA force field). Issues related to the compatibility between Berger and OPLS-AA force fields are described in ref.[41]. A set of simulations was carried out using reduced electrostatic charges on the ions; in this case, a charge of 0.7 e was used on the ions, as described in refs.[9,16]. Except for the ion force field, all simulation parameters (for non-bonded interactions, integration time step, thermostat, etc.) were identical to the parameters used in the Berger DPPC simulations described above.

All simulation files can be found at Ref. 42 for pure DPPC simulations, at Refs. 43,44 for simulations with ions, and at Refs. 14,15 for simulations with ions with scaled charges.

6.3.3 CHARMM36

POPC with NaCl: The simulation without ions is taken directly from Refs. 2,45. The starting structures for simulations with NaCl were made by replacing randomly located water molecules of the structure of pure POPC simulation with appropriate amount of ions. The force field for lipid were the same as in Refs. 2,45. The compatible TIP3P parameters for CHARMM36 and ion parameters with NBFIX by Venable et al.[11] were used. Simulations were ran with Gromacs 4.5.5 software[21]. Timestep of 2 fs was used with leap-frog integrator. Covalent bonds with hydrogens were constrained with LINCS algorithm[31,32]. Coordinates were written every 5 ps. PME with real space cut-off 1.4 nm was used for electrostatics. Lennard-Jones interactions were switched to zero between 0.8 nm and 1.2 nm. The neighbour list was updated every 5th step with cut-off 1.4 nm. Temperature was coupled separately for lipids and solution to 303 K with the velocity-rescale method[35] with coupling constant 0.2 ps. Pressure was semi-isotropically coupled to the atmospheric pressure with the Berendsen method[46].

Simulation without NBFIX[11] was ran with the same settings, except that the temperature was kept at 310 K with Nosé–Hoover[47,48] thermostat (simulation files available at Ref. 20).

POPC with $CaCl_2$: The starting structures with varying amounts of $CaCl_2$ were constructed using the CHARMM-GUI Membrane Builder (http://www.charmm-gui.org/) online tool[49]. All runs were performed with Gromacs 5.0.3 software package[22] and

CHARMM36 additive force field parameters for lipids[50] and ions were obtained from CHARMM-GUI input files. Simulation parameters provided by CHARMM-GUI were used. Particularly, the lengths of the bonds involving hydrogens were constrained with LINCS[31,32]. The temperatures of the lipids and the solvent were separately coupled to the Nose–Hoover[47,48] thermostat with a target temperature of 303 K and a relaxation time constant of 1.0 ps. Semi-isotropical pressure coupling to 1 bar was obtained with the Parrinello-Rahman barostat[36] with a time constant of 5 ps. Equations of motion were integrated with the Verlet algorithm[51] using a timestep of 2 fs. Long-range electrostatic interactions were calculated using the PME[33,34] method with a fourth order smoothing spline. A real space cut-off of 1.2 nm was employed with grid spacing of 0.12 nm in the reciprocal space. Lennard-Jones interactions were smoothly switched to zero between 1.0 nm and 1.2 nm. Verlet cutoff-scheme[51] was used with the long-range neighbour list updated every 20 steps. Coordinates were written every 10 ps. After energy minimisation and an equilibration run of 0.5 ns, 200 ns simulations were ran and the last 100 ns of each simulation was employed for the analysis.

DPPC with $CaCl_2$ (Yoo model): The systems contained 128 DPPC lipids and about 7600 TIP3P[52] water molecules, and an appropriate amount of ions as indicated in Table 1 in the main text. We have used CHARMM36 additive force field parameters for lipids[50] with compatible TIP3P water model. In the calcium model developed recently by Yoo et al.[1], each cation is decorated by seven hydrating water molecules (with different charges from the usual TIP3P), which are constrained to remain in its vicinity. The associated parameter files are available on `http://bionano.physics.illinois.edu/CUFIX`. The constraint on the calcium-oxygen distances was imposed by adding extra bonds through a harmonic potential $V(r) = k(r - r_0)^2$, with $r_0 = 2.25$ Å and $k = 10$ kcal·mol^{-1}·Å^{-2}.

The starting configuration of hydrated lipidic bilayers were constructed using *packmol*[53] with a large area per lipid (74 Å^2). After a first energy minimisation (5000 steps), varying amounts of Ca^{2+} and Cl^- ions were added by replacing water molecules, using the *autoionize* plugin of vmd package[54], mentioning explicitly the number of ions required. Ion placement is random, with the constraint of minimum 5 Å between ions and lipids, as well as between any two ions. A second energy minimisation was performed after inserting the ions.

All the minimisation and dynamics were conducted using the NAMD package[23]. The temperature of the whole system was controlled with Langevin thermostat with a target temperature of 323 K and a relaxation time constant of 1 ps. The modified NAMD version of Nose–Hoover barostat with Langevin dynamics (piston period of 0.1 ps and piston decay time of 0.05 ps) was used semi-isotropically for an average target pressure of 1 bar and an average zero surface tension. The equations of motion were integrated using the multiple time step Verlet r-RESPA algorithm[51] with a time step of 2 fs, and electrostatic forces calculated only every two time steps. Covalent bonds between heavy and hydrogen atoms were constrained using SHAKE/RATTLE algorithm. Long-range electrostatic interactions were calculated using the PME[33,34] method with a 4-th order smoothing spline and a grid spacing of about 0.1 nm. A cut-off of 1.2 nm was employed for the Lennard-Jones interactions, with a force-based switching function for distances beyond 1 nm. Neighbour lists with a radius of 1.4 nm were updated every 10 timesteps. Coordinates were written every 20 ps. After energy minimisation, a run of 200 ns simulations was performed, and the last $\sim$ 170 ns of trajectory was employed for the analysis. Error bars are defined by $\pm$ the standard error of the mean, taking into account the correlation time of the average order parameters (200 ps for 430 mM and 400 ps for 890 mM).

6.3.4 MacRog

The simulation parameters are identical to those employed in our earlier study[2] for the full hydration and dehydration simulations. The initial structures with varying amounts of NaCl were constructed from an extensively hydrated bilayer by replacing water molecules with ions using the Gromacs *genion* tool[55]. Even at the highest considered salt concentration, the amount of water molecules per lipid after this replacement process was still greater than 50.

6.3.5 Orange

The systems contained 72 POPC lipids and 2880 SPC water molecules, and an appropriate amount of ions as indicated in Table 1 in the main text.

For the lipids, we used an unpublished force field coined Orange force field. Briefly, this includes most bonded interactions from Berger lipids[28], except for dihedrals which were derived via *ab initio* calculations on small model compounds. As in Berger lipids, Lennard-Jones parameters are from OPLS[56–60]. Partial charges were derived on the basis of *ab initio* calculations. In simulations with ions, the Åqvist parameters were used[40]. The electrostatics were handled with PME[33,34], with real-space Coulomb cut-off set at 1.8 nm. Lennard-Jones potentials were cut off at 1.8 nm. The neighbour lists for the calculation of non-bonded forces were updated every 5 steps.

Temperature was set to 298K with the velocity-rescale thermostat[35] using a coupling constant of 0.1 ps^{-1}, and the pressure was set to 1 bar using the Berendsen weak coupling algorithm[46] (compressibility of $4.5{\cdot}10^{-5}$ bar^{-1}, time constant of 1 ps), coupling separately the x-y dimension and the z dimension to obtain a tensionless system. A time step of 2 fs was used for the integration (with the leap-frog algorithm), coordinates were written every 100 ps, and the total simulation time was 60 ns.

Simulation files for pure lipid simulations are found at Ref. 61 and for the simulations with ions at Refs. 62–65.

6.3.6 Slipids

DPPC: The simulation without ions from Ref. 2, available at Ref. 66, was used. For the simulation with 150 mM NaCl, the starting DPPC lipid bilayer, which was built with the online CHARMM-GUI[49] (http://www.charmm-gui.org/), contained 600 lipids hydrated by 30 water molecules per lipid.

For the simulation with 850 mM NaCl, the configuration from Ref. 66 was taken and an appropriate amount of water molecules was converted to ions to form a neutral NaCl solution. The simulation files are available at Ref. 67. Ion parameters by Roux[68,69],

TIP3P water model[52] and Stockholm lipids (Slipids) parameters[70,71] for phospholipids were used. GROMACS software package version 4.5.5 or 5.0.7[21] was employed for all simulations. After energy minimisation and a short equilibration run of 50 ps (time step 1 fs), 100 ns production runs were performed using a time step of 2 fs with leap-frog integrator. All covalent bonds were constrained with the LINCS[31,32] algorithm. Coordinates were written every 100 ps. PME[33,34] with real space cut-off at 1.0 nm was used for Coulomb interactions. Lennard-Jones interactions were switched to zero between 1.0 nm and 1.4 nm. The neighbour lists were updated every 10th step with a cut-off of 1.6 nm. Temperature was coupled separately for upper and bottom leaflets of the lipid bilayer, and for water to 323 K with the Nosé-Hoover thermostat[47,48] using a time constant of 0.5 ps. Pressure was semi-isotropically coupled to the atmospheric pressure with the Parrinello-Rahman[36] barostat using a time constant of 10 ps.

POPC: The simulation without ions from Ref. 2, available at Ref. 72 was used.
POPC with NaCl: A POPC bilayer consisting of 200 lipids, hydrated with 45 water molecules per lipid, was simulated in the presence of 130 mM NaCl. The Slipids model[70,71] was employed for lipids, the TIP3P model[52] for water, and the ion parameters by Smith and Dang[73] for NaCl. The system was first equilibrated for 5 ns with a time step of 1 fs after which a 100 ns production run was performed using a time step of 2 fs. Trajectories were written every 100 ps. The system was kept in a tensionless state at 1 bar using a semi-isotropic Parrinello–Rahman barostat[36] with a time constant of 1 ps. The temperature was maintained at 310 K with the velocity rescaling thermostat[35]. The time constant was set to 0.5 ps for both lipids and solvent (water and ions) which were coupled separately. Non-bonded interactions were calculated within a neighbour list with a radius of 1 nm and an update interval of 10 steps. The Lennard-Jones interactions were cut-off at 1 nm, whereas PME[33,34] was employed for long-range electrostatics. Dispersion correction was applied to both energy and pressure. All bonds were constrained with the LINCS[31,32]. algorithm.
POPC with $CaCl_2$: A POPC bilayer consisting of 200 lipids, hydrated with 45 water molecules per lipid, was simulated in the presence of 450 mM $CaCl_2$. The system was ran for 2000 ns and the last 100 ns was used for analysis. Other details are as in POPC with NaCl.

6.3.7 Lipid14

The starting structures with varying amounts of ions were constructed using the CHARMM-GUI Membrane Builder (http://www.charmm-gui.org/) online tool[49]. The GROMACS compatible force field parameters generated in Ref. 2 and available at Ref. 74 were used. The TIP3P water model[52] was used to solvate the system and Åqvist[40] parameters were used for ions. All runs were performed with Gromacs 5.0.3 software package[22] and LIPID14 force field parameters for POPC[75].

H-bond lengths were constrained with LINCS[31,32]. The temperatures of the lipids and the solvent were separately coupled to the Nose–Hoover[47,48] thermostat with a target temperature of 298.15 K and a relaxation time constant of 0.1 ps. Semi-isotropic pressure coupling to 1 bar was obtained with the Parrinello-Rahman barostat[36] with a time constant of 2 ps. Equations of motion were integrated with the Verlet algorithm[51] using a timestep of 2 fs. Long-range electrostatic interactions were calculated using the PME[33,34] method with a fourth order smoothing spline. A real space cut-off at 1.0 nm was employed with grid spacing of 0.12 nm in the reciprocal space. Lennard-Jones potentials were cut-off at 1 nm, with a dispersion correction applied to both energy and pressure. Verlet cutoff-scheme[51] were used with the long-range neighbour list updated every 20 steps. Coordinates were written every 10 ps.

After energy minimisation and an equilibration run of 5 ns, 200 ns production runs were performed and analysed. In case of the $CaCl_2$ systems only the last 100 ns of each simulation was employed for the analysis.

6.3.8 Ulmschneiders

The starting structures with varying amounts of ions were constructed using the CHARMM-GUI Membrane Builder (`http://www.charmm-gui.org`) online tool[49]. The force field parameters were obtained from Lipidbook[76]. The TIP3P water model[52] was used to solvate the system. Additionally, the simulations of ion-free bilayer were repeated with both Verlet and Group cutoff-schemes[77]. There was no significant difference in headgroup or glycerol backbone order parameters between these cutoff-schemes. All runs were performed with Gromacs 5.0.3 software package[22]. The glycerol backbone order parameters without ions were not the same as reported in the previous study[2]. The origin of discrepancy was located to the different initial structures which was taken from CHARMM-GUI in this work and from Lipidbook in the previous work. Since the order parameters with the initial structure from CHARMM-GUI are closer to the experimental values, the results indicate that the structure available from Lipidbook is stuck to a state with incorrect glycerol backbone structure, for more discussion see `https://github.com/NMRLipids/lipid_ionINTERACTION/issues/8`.

All-bond lengths were constrained with LINCS[31,32]. The temperatures of the lipids and the solvent were separately coupled to the Nose–Hoover[47,48] thermostat with a target temperature of 298.15 K and a relaxation time constant of 0.1 ps. Semi-isotropic pressure coupling to 1 bar was obtained with the Parrinello-Rahman barostat[36] with a time constant of 2 ps. Equations of motion were integrated with the Verlet algorithm[51] using a timestep of 2 fs. Long-range electrostatic interactions were calculated using the PME[33,34] method with a fourth order smoothing spline. A real space cut-off at 1.0 nm was employed with grid spacing of 0.12 nm in the reciprocal space. Lennard-Jones potentials were cut-off at 1 nm, with a dispersion correction applied to both energy and pressure. Verlet cutoff-scheme[51] were used with the long-range neighbour list updated every 20 steps. Coordinates were written every 10 ps. After energy minimisation and an equilibration run of 5 ns, 200 ns simulations were ran and the last 100 ns of each simulation was employed for the analysis.

7 Author Contributions

Andrea Catte
Mykhailo Girych ran and analysed several simulations. Discussed the project actively with OHSO.
Matti Javanainen provided data with several lipid and ion models. Discussed the project actively with OHSO. Supervised the work of JT.
Claire Loison provided results for CHARMM36 DPPC+$CaCl_2$ with Yoo's model.
Josef Melcr performed and analysed several simulations; discussed the project actively; corrected and contributed to the manuscript.
Markus S. Miettinen co-designed the project with OHSO. Provided the Berger DMTAP/DMPC trajectories. Performed the analysis of ΔS_{CH} as a function of bound charge.
Luca Monticelli
Jukka Määttä ran and analysed several simulations. Discussed the project actively in the blog.
Vasily S. Oganesyan
O. H. Samuli Ollila co-designed the project with MSM and managed the work. Ran and analysed several simulations. Wrote the manuscript.
Joona Tynkkynen
Sergey Vilov provided results for CHARMM36 DPPC+$CaCl_2$ with Yoo's model.

References

1 J. Yoo, J. Wilson and A. Aksimentiev, *Biopolymers*, 2016.

2 A. Botan, F. Favela-Rosales, P. F. J. Fuchs, M. Javanainen, M. Kanduč, W. Kulig, A. Lamberg, C. Loison, A. Lyubartsev, M. S. Miettinen, L. Monticelli, J. Määttä, O. H. S. Ollila, M. Retegan, T. Róg, H. Santuz and J. Tynkkynen, *J. Phys. Chem. B*, 2015, **119**, 15075–15088.

3 M. S. Miettinen, A. A. Gurtovenko, I. Vattulainen and M. Karttunen, *J. Phys. Chem. B*, 2009, **113**, 9226–9234.

4 M. S. Miettinen, *Molecular dynamics simulation trajectory of a fully hydrated DMPC lipid bilayer*, 2013, http://dx.doi.org/10.5281/zenodo.51635.

5 M. S. Miettinen, *Molecular dynamics simulation trajectory of a cationic lipid bilayer: 6/94 mol% DMTAP/DMPC*, 2016, http://dx.doi.org/10.5281/zenodo.51639.

6 M. S. Miettinen, *Molecular dynamics simulation trajectory of a cationic lipid bilayer: 50/50 mol% DMTAP/DMPC*, 2016, http://dx.doi.org/10.5281/zenodo.51748.

7 P. G. Scherer and J. Seelig, *Biochemistry*, 1989, **28**, 7720–7728.

8 C. M. Franzin, P. M. Macdonald, A. Polozova and F. M. Winnik, *Biochim. Biophys. Acta - Biomembranes*, 1998, **1415**, 219 – 234.

9 I. Leontyev and A. Stuchebrukhov, *Phys. Chem. Chem. Phys.*, 2011, **13**, 2613–2626.

10 M. Kohagen, P. E. Mason and P. Jungwirth, *J. Phys. Chem. B*, 2014, **118**, 7902–7909.

11 R. M. Venable, Y. Luo, K. Gawrisch, B. Roux and R. W. Pastor, *J. Phys. Chem. B*, 2013, **117**, 10183–10192.

12 J. Määttä, *DPPC_Berger_NaCl_scaled*, 2015, {http://dx.doi.org/10.5281/zenodo.16320}.

13 J. Määttä, *DPPC_Berger_NaCl_1Mol_scaled*, 2015, http://dx.doi.org/10.5281/zenodo.17228.

14 J. Määttä, *DPPC_Berger_OPLS06_NaCl_scaled*, 2015, {http://dx.doi.org/10.5281/zenodo.16485}.

15 J. Määttä, *DPPC_Berger_OPLS06_NaCl_1Mol_scaled*, 2015, http://dx.doi.org/10.5281/zenodo.17209.

16 M. Kohagen, P. E. Mason and P. Jungwirth, *J. Phys. Chem. B*, 2016, **120**, 1454–1460.

17 M. Javanainen, *POPC @ 310K, varying amounts of NaCl. Slipids with ECC-scaled ions*, 2015, http://dx.doi.org/10.5281/zenodo.35193.

18 M. Javanainen, *POPC @ 310K, 450 mM of CaCl_2. Charmm36 with ECC-scaled ions*, 2016, http://dx.doi.org/10.5281/zenodo.45008.

19 M. Javanainen, *POPC @ 310K, 450 mM of CaCl_2. Slipids with ECC-scaled ions*, 2016, http://dx.doi.org/10.5281/zenodo.45007.

20 J. Melcr, *Simulation files for POPC lipid membrane with Charmm36 force field without NBFIX for Gromacs MD simulation engine*, 2016, http://dx.doi.org/10.5281/zenodo.55318.

21 S. Pronk, S. Páll, R. Schulz, P. Larsson, P. Bjelkmar, R. Apostolov, M. R. Shirts, J. C. Smith, P. M. Kasson, D. van der Spoel, B. Hess and E. Lindahl, *Bioinformatics*, 2013, **29**, 845–854.

22 M. J. Abraham, T. Murtola, R. Schulz, S. Páll, J. C. Smith, B. Hess and E. Lindahl, *SoftwareX*, 2015, **1-2**, 19–25.

23 J. C. Phillips, R. Braun, W. Wang, J. Gumbart, E. Tajkhorshid, E. Villa, C. Chipot, R. D. Skeel, L. Kalé and K. Schulten, *J. Comput. Chem.*, 2005, **26**, 1781–1802.

24 D. van der Spoel, E. Lindahl, B. Hess, A. R. van Buuren, E. Apol, P. J. Meulenhoff, D. P. Tieleman, A. L. T. M. Sijbers, K. A. Feenstra, R. van Drunen and H. J. C. Berendsen, *GROMACS user manual version 4.0*, 2005.

25 O. H. S. Ollila and et al., 2015, https://github.com/NMRLipids/lipid_ionINTERACTION.

26 T. M. Ferreira, F. Coreta-Gomes, O. H. S. Ollila, M. J. Moreno, W. L. C. Vaz and D. Topgaard, *Phys. Chem. Chem. Phys.*, 2013, **15**, 1976–1989.

27 O. H. S. Ollila, T. Ferreira and D. Topgaard, *MD simulation trajectory and related files for POPC bilayer (Berger model delivered by Tieleman, Gromacs 4.5)*, 2014, {http://dx.doi.org/10.5281/zenodo.13279}.

28 O. Berger, O. Edholm and F. Jähnig, *Biophys. J.*, 1997, **72**, 2002 – 2013.

29 M. Bachar, P. Brunelle, D. P. Tieleman and A. Rauk, *J. Phys. Chem. B*, 2004, **108**, 7170–7179.

30 T. P. Straatsma and H. J. C. Berendsen, *J. Chem. Phys*, 1988, **89**, year.

31 B. Hess, H. Bekker, H. J. C. Berendsen and J. G. E. M. Fraaije, *J. Comput. Chem.*, 1997, **18**, 1463–1472.

32 B. Hess, *J. Chem. Theory Comput.*, 2008, **4**, 116–122.

33 T. Darden, D. York and L. Pedersen, *J. Chem. Phys*, 1993, **98**, year.

34 U. L. Essman, M. L. Perera, M. L. Berkowitz, T. Larden, H. Lee and L. G. Pedersen, *J. Chem. Phys.*, 1995, **103**, 8577–8592.

35 G. Bussi, D. Donadio and M. Parrinello, *J. Chem. Phys*, 2007, **126**, year.

36 M. Parrinello and A. Rahman, *J. Appl. Phys.*, 1981, **52**, 7182–7190.

37 J. Määttä, *DPPC_Berger*, 2015, http://dx.doi.org/10.5281/zenodo.13934.

38 J. Määttä, *DPPC_Berger_NaCl*, 2015, http://dx.doi.org/10.5281/zenodo.16319.

39 J. Määttä, *DPPC_Berger_NaCl_1Mol*, 2015, http://dx.doi.org/10.5281/zenodo.17210.

40 J. Åqvist, *J. Phys. Chem.*, 1990, **94**, 8021–8024.

41 D. P. Tieleman, J. L. MacCallum, W. L. Ash, C. Kandt, Z. Xu and L. Monticelli, *J. Phys. Condens. Matter*, 2006, **18**, S1221.

42 J. Määttä, *DPPC_Berger_OPLS06*, 2015, http://dx.doi.org/10.5281/zenodo.17237.

43 J. Määttä, *DPPC_Berger_OPLS06_NaCl*, 2015, http://dx.doi.org/10.5281/zenodo.16484.

44 J. Määttä, *DPPC_Berger_OPLS06_NaCl_1Mol*, 2016, http://dx.doi.org/10.5281/zenodo.46152.

45 O. H. S. Ollila and M. Miettinen, *MD simulation trajectory and related files for POPC bilayer (CHARMM36, Gromacs 4.5)*, 2015, {http://dx.doi.org/10.5281/zenodo.13944}.

46 H. J. C. Berendsen, J. P. M. Postma, W. F. van Gunsteren, A. DiNola and J. R. Haak, *J. Chem. Phys.*, 1984, **81**, 3684–3690.

47 S. Nose, *Mol. Phys.*, 1984, **52**, 255–268.

48 W. G. Hoover, *Phys. Rev. A*, 1985, **31**, 1695–1697.

49 J. Lee, X. Cheng, J. M. Swails, M. S. Yeom, P. K. Eastman, J. A. Lemkul, S. Wei, J. Buckner, J. C. Jeong, Y. Qi, S. Jo, V. S. Pande, D. A. Case, I. Charles L. Brooks, J. Alexander D. MacKerell, J. B. Klauda and W. Im, *J. Chem. Theory Comput.*, 2016, **12**, 405–413.

50 J. B. Klauda, R. M. Venable, J. A. Freites, J. W. O'Connor, D. J. Tobias, C. Mondragon-Ramirez, I. Vorobyov, A. D. M. Jr and R. W. Pastor, *J. Phys. Chem. B*, 2010, **114**, 7830–7843.

51 S. Páll and B. Hess, *Computer Physics Communications*, 2013, **184**, 2641 – 2650.

52 W. L. Jorgensen, J. Chandrasekhar, J. D. Madura, R. W. Impey and M. L. Klein, *J. Chem. Phys*, 1983, **79**, year.

53 L. Martínez, R. Andrade, E. G. Birgin and J. M. Martínez, *J. Comput. Chem.*, 2009, **30**, 2157–2164.

54 W. Humphrey, A. Dalke and K. Schulten, *J. Mol. Graphics*, 1996, **14**, 33–38.

55 M. Abraham, D. van der Spoel, E. Lindahl, B. Hess and the GROMACS development team, *GROMACS user manual version 5.0.7*, 2015.

56 W. L. Jorgensen, J. D. Madura and C. J. Swenson, *J. Am. Chem. Soc.*, 1984, **106**, 6638–6646.

57 W. L. Jorgensen and J. Gao, *J. Phys. Chem.*, 1986, **90**, 2174–2182.

58 W. L. Jorgensen, *J. Phys. Chem.*, 1986, **90**, 1276–1284.

59 W. L. Jorgensen and J. Tirado-Rives, *J. Am. Chem. Soc.*, 1988, **110**, 1657–1666.

60 J. M. Briggs, T. B. Nguyen and W. L. Jorgensen, *J. Phys. Chem.*, 1991, **95**, 3315–3322.

61 O. H. S. Ollila, J. Määttä and L. Monticelli, *MD simulation trajectory for POPC bilayer (Orange, Gromacs 4.5.)*, 2015, http://dx.doi.org/10.5281/zenodo.34488.

62 O. H. S. Ollila, J. Määttä and L. Monticelli, *MD simulation trajectory for POPC bilayer with 140mM NaCl (Orange, Gromacs 4.5.)*, 2015, http://dx.doi.org/10.5281/zenodo.34491.

63 O. H. S. Ollila, J. Määttä and L. Monticelli, *MD simulation trajectory for POPC bilayer with 510mM NaCl (Orange, Gromacs 4.5.)*, 2015, http://dx.doi.org/10.5281/zenodo.34490.

64 O. H. S. Ollila, J. Määttä and L. Monticelli, *MD simulation trajectory for POPC bilayer with 510mM CaCl_2 (Orange, Gromacs 4.5.)*, 2015, http://dx.doi.org/10.5281/zenodo.34498.

65 S. Ollila, J. Määttä and L. Monticelli, *MD simulation trajectory for POPC bilayer with 1000mM NaCl (Orange, Gromacs 4.5.)*, 2015, http://dx.doi.org/10.5281/zenodo.34497.

66 J. Määttä, *DPPC_Slipids*, 2014, http://dx.doi.org/10.5281/zenodo.13287.

67 J. Melcr, *Simulation files for DPPC lipid membrane with Slipids force field for Gromacs MD simulation engine*, 2016, http://dx.doi.org/10.5281/zenodo.55322.

68 D. Beglov and B. Roux, *J. Chem. Phys.*, 1994, **100**, 9050–9063.

69 B. Roux, *Biophys. J.*, 1996, **71**, 3177 – 3185.

70 J. P. M. Jämbeck and A. P. Lyubartsev, *J. Phys. Chem. B*, 2012, **116**, 3164–3179.

71 J. P. M. Jämbeck and A. P. Lyubartsev, *J. Chem. Theory Comput.*, 2012, **8**, 2938–2948.

72 M. Javanainen, *POPC @ 310K, Slipids force field.*, 2015, DOI: 10.5281/zenodo.13887.

73 D. E. Smith and L. X. Dang, *J. Chem. Phys*, 1994, **100**, year.

74 O. H. S. Ollila and M. Retegan, *MD simulation trajectory and related files for POPC bilayer (Lipid14, Gromacs 4.5)*, 2014, http://dx.doi.org/10.5281/zenodo.12767.

75 C. J. Dickson, B. D. Madej, Ã. A. Skjevik, R. M. Betz, K. Teigen, I. R. Gould and R. C. Walker, *J. Chem. Theory Comput.*, 2014, **10**, 865–879.

76 J. Domański, P. Stansfeld, M. Sansom and O. Beckstein, *J. Membr. Biol.*, 2010, **236**, 255–258.

77 M. Girych and O. H. S. Ollila, *POPC_Ulmschneider_OPLS_Verlet_Group*, 2015, http://dx.doi.org/10.5281/zenodo.30904.